

Accepted Manuscript

Immobilisation of Iron tris(β -diketonates) on a two-dimensional flat amine functionalized silicon wafer: A catalytic study of the formation of urethane, from ethanol and a diisocyanate derivative

M.M. Conradie, J. Conradie, E. Erasmus

PII: S0277-5387(14)00274-5

DOI: <http://dx.doi.org/10.1016/j.poly.2014.04.054>

Reference: POLY 10698

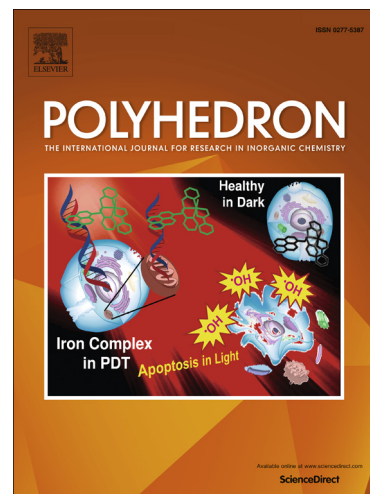
To appear in: *Polyhedron*

Received Date: 7 March 2014

Accepted Date: 27 April 2014

Please cite this article as: M.M. Conradie, J. Conradie, E. Erasmus, Immobilisation of Iron tris(β -diketonates) on a two-dimensional flat amine functionalized silicon wafer: A catalytic study of the formation of urethane, from ethanol and a diisocyanate derivative, *Polyhedron* (2014), doi: <http://dx.doi.org/10.1016/j.poly.2014.04.054>

This is a PDF file of an unedited manuscript that has been accepted for publication. As a service to our customers we are providing this early version of the manuscript. The manuscript will undergo copyediting, typesetting, and review of the resulting proof before it is published in its final form. Please note that during the production process errors may be discovered which could affect the content, and all legal disclaimers that apply to the journal pertain.



Manuscript

Immobilisation of Iron tris(β -diketonates) on a two-dimensional flat amine functionalized silicon wafer: A catalytic study of the formation of urethane, from ethanol and a diisocyanate derivative

M. M. Conradie, J. Conradie and E. Erasmus*

Department of Chemistry, University of the Free State, Bloemfontein, 9300, Republic of South Africa.

Contact author details:

Name: Elizabeth Erasmus

Tel: ++27-51-4019656

Fax: ++27-51-4446384

e-mail: erasmuse@ufs.ac.za

Immobilisation of Iron tris(β -diketonates) on a two-dimensional flat amine functionalized silicon wafer: A catalytic study of the formation of urethane from ethanol and a diisocyanate derivative

M. M. Conradie, J. Conradie and E. Erasmus*

Department of Chemistry, University of the Free State, Bloemfontein, 9300, Republic of South Africa.

Abstract

A series of immobilized iron tris(β -diketonato) catalysts on a Si-wafer was prepared, by covalently anchoring the $\text{Fe}(\beta\text{-diketonato})_3$ complexes [where $\beta\text{-diketonato} = (\text{RCOCHCOR}')^-$, with **1** = acac ($\text{R} = \text{CH}_3$; $\text{R}' = \text{CH}_3$), **2** = dbm ($\text{R} = \text{C}_6\text{H}_5$; $\text{R}' = \text{C}_6\text{H}_5$), **3** = tfaa ($\text{R} = \text{CH}_3$; $\text{R}' = \text{CF}_3$), and **4** = hfaa ($\text{R} = \text{CF}_3$; $\text{R}' = \text{CF}_3$)], onto an aminated functionalised Si-wafer. These new catalysts were characterised by X-ray photo-electron spectroscopy (XPS) and atomic force microscopy (AFM). XPS data revealed that ca. 27 - 91% of all the amine groups anchored the catalyst, $\text{Fe}(\beta\text{-diketonato})_3$. Different Gaussian peaks could be fitted into the F 1s peak, due to the fluorine either being positioned adjacent to the -C-O-Fe-, or to the -C-N-Fe-. The binding energy of the Fe $2p_{3/2}$ peak varied between ca. 710.4 and 711.0 eV, depending on the electron donating properties of the R-groups on the β -diketonato ligands, expressed as the sum of the Gordy group electronegativities of the R-groups in the β -diketonato ligands. The AFM photographs showed that the surface changed dramatically after each treatment: after amination

(binding of the aminate silane onto the hydroxylate Si-wafer) the Si-wafer turned from flat with a few spikes, to a very wavy surface with smooth lumps. The surface topography again changed, after covalent anchoring of the iron tris(β -diketonato) complexes, to a nodular surface with poorly defined grain boundaries. These immobilized iron tris(β -diketonato) on Si-wafer catalysts, were evaluated for their catalytic activity, during the formation of hexamethylenediurethane from hexamethylenediisocyanate and ethanol. The TOF varied between 15 – 46 s⁻¹, depending on the electron donating properties of the R-groups on the β -diketonato ligands. The more electron donating the R groups, the higher the TOF.

Keywords: iron β -diketonates, catalysis, urethane, XPS, group electronegativity

1. Introduction

Immobilisation of homogeneous catalysts onto a solid support has recently enjoyed much attention due to the high selectivity and activity of the homogeneous part and the recoverability and stability of the heterogeneous part. One of the many different ways to immobilise the homogeneous catalyst onto the solid support, is by wet impregnation (or the two-dimensional version, namely spin coating) of the homogeneous catalyst onto the solid support,¹ in which case the homogeneous catalyst is fixed onto the surface by means of Van der Waals forces. The homogeneous catalyst however, can also be anchored onto the surface by means of a ligand exchange type of reaction,² but the most popular anchoring procedure is by covalently anchoring the metal complex onto the solid

support.³ This normally is achieved, by linking a functionalised silane to the solid support (via a silicon-ether type of bond) with an appropriate functional group on the other side, where the metal complex easily can bind to. Functional groups which have been used to anchor the metal complexes are amines,⁴ phosphines,⁵ allyls,⁶ and thiols,⁷ to name a few. The covalent anchoring of the homogeneous catalyst metal complex is favoured, since the linkage is stable towards most solvents, which still allows for the high selectivity of the catalyst, but also introduces recoverability. Iron complexes are known in nature for their importance in electron transfer processes,⁸ oxygen transfer reactions,⁹ substitution and reduction,¹⁰ but here we focus on iron-acetonato complexes. Metal acetylacetonato complexes have materialized as versatile catalysts for a wide range of different reactions, including enantioselective catalysis,¹¹ acetylation,¹² oxidative coupling of naphthol,¹³ oxidation,^{4d,14} and polymerisation.¹⁵ The catalytic formation of urethane, as a representation for the catalytic formation of polyurethane by the homogeneous $\text{Fe}(\text{acac})_3$ complex, has been shown to be very efficient, with a turnover rate of 74.2 h^{-1} in comparison with the commercially available catalyst, dibutyltin dilaurate (DBTDL), which has a turnover rate of 29.5 h^{-1} .¹⁶

In this publication, we describe the preparation and characterisation of the immobilized homogeneous catalyst $\text{Fe}(\beta\text{-diketonato})_3$, on an aminated flat two dimensional silicon wafer (as model catalyst) for a series of β -diketonato-ligands containing different electronic properties. The catalytic formation of the urethane derivative, *N,N*-1,6-hexanediylbis-*C,C*-diethyl ester (hexamethylenediurethane), obtained from the reaction between hexamethylenediisocyanate (HDI) and ethanol (EtOH), to mimic the catalytic formation of polyurethane by this immobilized iron catalyst, is also described. Different

immobilized $\text{Fe}(\beta\text{-diketonato})_3$ heterogeneous catalysts [with β -diketonato = acetylacetonato (acac, **1**), dibenzoylmethane (dbm, **2**), trifluoroacetylacetonato, (tfaa, **3**) and hexafluoroacetylacetonato (hfaa, **4**)] will be compared to each other and to their homogeneous counter parts.

2. Experimental

2.1. Chemicals and instruments

Ethanol, iron nitrate and β -diketones were purchased from Aldrich or Merck, and were used without any further purification. Silicon wafers were obtained from Topsil, these are n-type, single crystalline of (100) orientation, with resistivity of 370-410 $\Omega\cdot\text{m}$. Attenuated total reflectance Fourier transformed infra-red (ATR FTIR) spectra were recorded on a Bruker Tensor 27 infrared spectrophotometer, fitted with a Pike MIRacle single bounce, and a diamond ATR. Atomic force microscopy was performed on a Shimadzu SPM – 9600, with a 125 μm scanner. X-ray photoelectron spectroscopy (XPS) data was recorded on a PHI 5000 Versaprobe system, with monochromatic Al $K\alpha$ X-ray source. Spectra were obtained, using the aluminium anode (Al $K\alpha$ = 1486.6 eV), operating at 50 μm , 12.5 W and 15 kV energy (97 X-ray beam). The survey scans were recorded at constant pass energy of 187.85 eV, and the detailed region scans at constant pass energy of 29.35 eV, with the analyzer resolution being ≤ 0.5 eV. The background pressure was 2×10^{-6} Pa. The XPS data was analysed, utilizing Multipak version 8.2c computer software,¹⁷ applying Gaussian–Lorentz fits (the Gaussian/Lorentz ratios were always $> 95\%$).

2.2. Synthesis of tris(β -diketonato)iron(III) complexes, $[Fe^{III}(\beta\text{-diketonato})_3]$, **1-4**

Four complexes, $[Fe^{III}(\beta\text{-diketonato})_3]$, **1-4**, were prepared by the following general procedure¹⁸ adapted from literature.¹⁹

A metal solution of 0.15 mmol $Fe(NO_3)_3 \cdot 9H_2O$, was buffered with 0.45 mmol $CH_3COONa \cdot 3H_2O$ (dissolved in 10 ml water). Ethanol was added to this solution, to produce an 1:1 volume ratio water:ethanol solution. 0.53 mmol of the relevant β -diketone was added [if the β -diketone was a liquid (Htfaa and Hhfaa), it was added as is, while the solid β -diketone (Hacac and Hdbm) was dissolved in 10 ml dichloromethane (DCM), before addition]. The resulting solution was stirred for 30 min, and left to stand overnight (in a fume hood), allowing slow evaporation of the solvent. The precipitate was collected by filtration and washing with water.

2.2.1. Characterization data for $[Fe(CH_3COCHCOCH_3)_3]$, **1** $Fe(acac)_3$

Yield 73%. M.p. 180-182 °C (reported: 179 °C,²⁰ 180 °C²¹). UV: λ_{max} 270 nm, ϵ_{max} 25842 $mol^{-1} \cdot dm^3 \cdot cm^{-1}$ (CH_3CN). MS Calcd. ($[M]^+$, positive mode): m/z 352.2. Found: m/z 351.9. Anal. Calcd. for $FeC_{15}H_{21}O_6$: C, 51.01; H, 5.99. Found: C, 50.42; H, 5.91.

2.2.2. Characterisation data for $[Fe(C_6H_5COCHCOC_6H_5)_3]$, **2** $Fe(dbm)_3$

Yield 71%. M.p. 264-265.2 °C (reported: 261 °C,²² 257 °C²³). UV: λ_{max} 336 nm, ϵ_{max} 48608 $mol^{-1} \cdot dm^3 \cdot cm^{-1}$ (CH_3CN). MS Calcd. ($[M]^+$, positive mode): m/z 725.6. Found: m/z 725.3. Anal. Calcd. for $FeC_{45}H_{33}O_6$: C, 74.49; H, 4.58. Found: C, 75.29; H, 4.51.

2.2.3. Characterisation data for $[Fe(CH_3COCHCOCF_3)_3]$, **3** $Fe(tfaa)_3$

Yield 91%. M.p. 113.5-116.1 °C (reported: 115 °C^{20,24}). UV: λ_{\max} 271 nm, ϵ_{\max} 48996 mol⁻¹.dm³.cm⁻¹ (CH₃CN). MS Calcd. ([M]⁻, negative mode): m/z 514.1. Found: m/z 513.5. Anal. Calcd. for FeC₁₅H₁₂O₆F₉: C, 34.98; H, 2.35. Found: C, 34.48; H, 2.30.

2.2.4. Characterisation data for [Fe(CF₃COCHCOCF₃)₃], 4 Fe(hfaa)₃

Yield 51%. M.p. 56-58 °C (reported: 55 °C²⁵). MS Calcd. ([M]⁻, negative mode): m/z 677.0. Found: m/z 676.8. Anal. Calcd. for FeC₁₅H₃O₆F₁₈: C, 26.61; H, 0.45. Found: C, 26.17; H, 0.51.

2.3. Preparation of Si-wafers, bearing 4-6 OH groups/nm^{2,26,27}

A silicon wafer was cut into size, ca. 2 x 2 cm, and calcined in air, at 750 °C for 24 h, forming an amorphous 90 nm SiO₂ over-layer. It was then submerged into a 1:1 (v/v) mixture of H₂O₂ (25% solution) and NH₄OH (35% solution), at room temperature. Subsequently, the Si-wafers were kept submerged for 1 h in boiling doubly distilled water, before being left to dry for 16 h. The wafers treated in this manner, acquired 4 - 6 -OH functional groups / nm^{2,26,27}. The surface density of OH groups (the silanol number) is a physicochemical constant for a fully hydroxylated surface and does not change upon exposure to air.²⁷

2.4. Anchoring of 3-aminopropyltrimethoxysilane onto the silicon wafers^{4a}

3-Aminopropyltrimethoxysilane was covalently anchored onto the hydroxylated Si wafer surface as follows: The previously prepared wafers were immersed in a solution of 3-aminopropyltrimethoxysilane (500 mg) in dried toluene (20 ml), under gentle stirring for

60 h. These amino-functionalized wafers, were then washed three times with isopropanol in a sonic bath, and dried in a nitrogen stream.

2.5. Covalent binding of $[Fe^{III}(\beta\text{-diketonato})_3]$, **1-4**, onto aminated silicon wafers

The amino-functionalized wafer was cut into smaller pieces (**1**: 0.5 cm x 0.48 cm = 0.24 cm²; **2**: 0.5 cm x 0.52 cm = 0.26 cm²; **3**: 0.3 cm x 0.6 cm = 0.18 cm²; **4**: 0.45 cm x 0.46 cm = 0.21 cm²) and immersed in a 0.5 mol.dm⁻³ solution of the desired $[Fe^{III}(\beta\text{-diketonato})_3]$ complex, **1-4**, in toluene. This suspension was refluxed gently at 111 °C for ~ 16 h. The wafers were then removed from the solution, and washed three times with isopropanol. Finally, the obtained wafers were dried by a nitrogen stream. A catalyst loading of 0.5 – 2.7 Fe-complex molecules / nm² onto the silicon surface was obtained, as determined by atomic ratios from XPS data (see Table 3).

2.6. Catalytic formation of hexamethylenediurethane from hexamethylenediisocyanate and ethanol

The catalytic reactions were performed under an argon atmosphere, at 30 °C in a closed 10 ml reaction vessel. A 0.1 ml solution of 1 equivalent hexamethylenediisocyanate (HDI) and 10 equivalents ethanol (giving a HDI concentration of 0.22 mol.L⁻¹) was placed into the reaction vessel, in the absence of any other solvent, sufficient to cover the iron model catalytic Si-wafer of surface area ca. 25 mm², in a thin layer of HDI solution (see Figure 1). This thin layer of HDI was not stirred with a magnetic stirrer to prevent damage of the catalytic surface. Convection currents within the HDI solution ensured contact between the catalytic sites and the reactants. Small samples of the reaction

mixture were removed with a syringe (or Pasteur pipette) at specified times, and analysed by ATR FTIR. The catalytic behaviour of the different iron tris(β -diketonato)-model catalysts, were evaluated on the basis of turnover frequency. In order to test the stability of these catalysts, the catalytic reaction was repeated 8 times under the same conditions, after excessive washing of the catalyst with EtOH and acetone.

Figure 1. ABOUT HERE

3. Results and Discussion

Preparation of the catalyst

The synthesis of the $[\text{Fe}(\beta\text{-diketonato})_3]$ complexes, [where β -diketonato = $\text{RCOCHCOR}'$, with **1** = acac ($\text{R} = \text{CH}_3$; $\text{R}' = \text{CH}_3$), **2** = dbm ($\text{R} = \text{C}_6\text{H}_5$; $\text{R}' = \text{C}_6\text{H}_5$), **3** = tfaa ($\text{R} = \text{CH}_3$; $\text{R}' = \text{CF}_3$), and **4** = hfaa ($\text{R} = \text{CF}_3$; $\text{R}' = \text{CF}_3$)], involved the buffering of an aqueous solution of $\text{Fe}(\text{NO})_3 \cdot 9\text{H}_2\text{O}$ with sodium acetate. This buffering assists the next step of the reaction, which is the coordination of the β -diketone ligand onto the Fe. With the exception of complex **4** (51 %), all compounds produced good yields of 71 - 91 %.

The anchoring of these homogeneous catalyst, namely the $[\text{Fe}(\beta\text{-diketonato})_3]$ complexes (**1-4**) onto the two-dimensional solid support, is illustrated in Scheme 1. The preparation of the immobilized iron catalyst starts by modifying the two-dimensional silicon wafer. The silicon wafer with a (100) surface orientation, is calcined in air, to produce a thin amorphous -O-Si-O- layer on the surface of the Si. This surface is then hydrolyzed to yield ca. 4-6 silanol (Si-OH) groups per nm^2 , to become hydrophilic.^{26,27} These hydroxyl

groups provide a good anchoring point for covalent bonding of silanes, to form a silyl ether bond. 3-Aminopropyltrimethoxysilane, **5**,²⁸ was allowed to react with the hydroxyl groups on the modified silicon wafer, forming a silicon surface which is covered with a mono-aminated layer, surface **6**. The reaction between amino groups of surface **6** and the [Fe(β -diketonato)₃] complexes (**1-4**), results in the formation of amine bonds between the aminated silicon surface and the iron complex, producing surfaces **1a-4a**. These surfaces (**1a-4a**) were characterized by XPS and AFM, obtaining information on the metal content, the chemical environment of the atoms, and the morphology of the surfaces.

Scheme 1. ABOUT HERE

X-ray photoelectron spectroscopy (XPS) characterization

X-ray photo-electron spectroscopy (XPS) characterization of surfaces **1a-4a** was performed, obtaining information on the atomic ratios, binding energy and chemical environment of the silicon, iron, nitrogen and fluorine atoms. The binding energies of the elements detected on the surfaces **1a-4a**, were referenced according to the C 1s position at 284.90 eV and summarized in Table 1.

The Si 2p peaks

In all cases, the silicon Si 2p peak was resolved into three peaks, which were found to be between 100.74 and 103.83 eV for all four surfaces, **1a-4a**. The first peak at ca 101.5 eV, is assigned to $-\text{O}-\underline{\text{Si}}-\text{CH}_2$ ²⁹ of the silane, the second peak at ca.102.6 eV is assigned to $-\text{O}-\underline{\text{Si}}-\text{OH}$ while the peak at ca. 103.5 eV is related to the $-\text{O}-\underline{\text{Si}}-\text{O}-$ on the surface.³⁰ The ratio between the two different Si peaks detected, was ca. 1 : 1.97 : 0.48 (29% : 57% :

14%, see Table 1), showing that there are ca. one -O-Si-CH₂- group for every two -O-Si-OH groups, with no metallic silicon detected at 99 eV.

The N 1s peaks

For the surfaces where groups R = R' (**1a**, **2a** and **4a**), the N 1s peak (resulting from the amine silane, bound to the surface) could be resolved into two distinct peaks, while for surface **3a**, where R ≠ R', the N 1s peak was resolved into three different peaks. The N 1s peak at the higher binding energy (401.15 - 402.72 eV, see Table 1) is associated with the unreacted amino groups of the silane layer on the surface (Scheme 1); this is in agreement with literature.³¹ The N 1s peak at the lower binding energy (398.65 – 401.03 eV, see Table 1) is attributed to the amine group (Scheme 1), which covalently binds (anchors) the iron complexes onto the solid support.³² A possible rationalization for the wide range of binding energies associated with each assignment, could be the influence of the different R-groups on the β-diketonato ligands, which have different electron donating properties as expressed by the Gordy group electronegativities ($\chi_{\text{CF}_3} = 3.01$, $\chi_{\text{CH}_3} = 2.34$, $\chi_{\text{Ph}} = 2.21$),³³ which are known to greatly influence the chemical environment (chemical and physical properties) of the surrounding molecules,³⁴ which could cause these shifts in binding energies.

For surface **3a**, where R ≠ R', the N 1s peak could be resolved into two distinct peaks.

The fitted peak at the highest binding energy (401.95 eV), is assigned to the unbound nitrogen of the amine, due to it having similar binding energy with the other unbound nitrogen amines, as well as being in agreement with literature.³¹ The other two Gaussian fitted peaks at binding energies of 398.65 and 401.03 eV, are associated with the nitrogen atoms of the amine groups bound to the iron catalyst. The reason why there are two

separate peaks, (unlike with surfaces **1a**, **2a** and **4a**), is since for surface **3a**, the functional groups are not identical, $R \neq R'$. These different R-groups on the same ligand have very different Gordy group electronegativities ($\chi_{\text{CH}_3} = 2.34$ and $\chi_{\text{CF}_3} = 3.01$), which dramatically alter the chemical environment of the atoms surrounding them (Figure 2).³⁴ When the amine group is adjacent to the $-\text{CH}_3$ group (with $\chi_{\text{CH}_3} = 2.34$, which is electron donating), the binding energy will be lower (namely 398.65 eV) than the binding energy (401.03 eV) when the amine group is adjacent to the $-\text{CF}_3$ group (with $\chi_{\text{R}} = 3.01$, which is electron withdrawing); since the more electron withdrawing the effect the nitrogen atom experiences, the more tightly it will bind to its core electrons, leading to a higher binding energy.

Between 27 and 91% of the available amino groups react with the iron complexes, again depending on the different R groups (see Table 1). The low anchoring concentration in case of surface **2a** relative to the other surfaces, could possibly be attributed to steric hindrance of the phenyl groups that are larger than the CF_3 or CH_3 groups; after one Fe-complex reacted, it blocks other Fe-complexes from reacting with free amino groups in its close vicinity. Another possible explanation could be that there is hydrogen bonding between the free amino groups on the surface, causing them to clump together in long smooth lumps as can be seen from the AFM data (see Figure 5b). This association does not allow easy access for reaction with the Fe-complex to occur. Low anchoring of metal complex to these type of amino groups on a surface is quite common. For example, when $\text{Mn}(\text{acac})_3$ was reacted with 3-aminopropylsilica,¹⁴ ca. 50% anchoring occurred, while only 7 - 25% anchoring occurred during the anchoring of different metallocenylaldehydes onto amine-functionalized flat Si-surfaces.^{4a}

Figure 2. ABOUT HERE

The F 1s peaks

For the two catalysts with fluorine-containing ligands, namely surfaces **3a–4a**, multiple Gaussian fitted peaks again could be fitted into the F 1s peak. Surface **4a** showed only two F 1s peaks attributed to the fluorine of the CF₃ group, namely either the fluorine bound to the ether bond (-O-C-CF₃, see **4a^f** in Table 1) or the amine bond (-N-C-CF₃, see **4a^e** in Table 1), at binding energies of 688.27 and 684.69 eV respectively. The lower of these two binding energies is associated with the amine bond, since the Pauling electronegativity of the nitrogen atom is lower (3.04) than that for oxygen (3.44).³⁵

However, the F 1s peak of surface **3a**, was fitted with three different Gaussian peaks, one fitted peak for the two β -diketonato ligands, which are not involved in the amine bond and two fitted peaks for the β -diketonato ligand involved in the amine bond (Figure 2).

The two unequal R-groups on the β -diketonato ligand that are involved in the amine bond can cause two different binding modes, due to either the CF₃ or the CH₃ group being adjacent to the amine bond (Figure 2). The fitted peak at the lowest binding energy (684.63 eV) is associated with the amine bond (-CN-CF₃, see **3a^g** in Table 1) of the enaminone ligand (which bonds to the Fe metal via only one O and one N atom; and where the CF₃ group on the ligand is located *cis* to the Si surface, Figure 2 right). While the peak at intermediate energy (686.24 eV) is associated with the ether bond (-O-C-CF₃,

see **3a^h** in Table 1) of the same enaminone ligand (but where the CF₃ group on the ligand is located *trans* to the Si surface, Figure 2 left). This assignment was made, again considering the relative Pauling electronegativities of the oxygen and nitrogen atoms. The F 1s peak fitted at the highest binding energy (688.5 eV), is associated with the ether bond (-O-C-CF₃, see **3aⁱ** in Table 1) of the two β-diketonato ligands which are not involved in the amine bond (*i.e.* where the ligands bond to the Fe metal via two oxygen atoms). This interpretation gives a clearer understanding of the preferential binding of the fluorine-containing iron tris(β-diketonato) complexes onto the aminated silicon surface.

Figure 3. ABOUT HERE

The Fe 2p_{3/2} and 2p_{1/2} peaks

The Fe 2p_{3/2} peaks were found between 710.37 and 710.94 eV, while the Fe 2p_{1/2} peaks were found 13.95 eV higher; see Figure 3 for surface **3a** as an example. A plot of the sum of the Gordy group electronegativities of the R-groups on the β-diketonato ligands, *vs* the binding energy of the Fe 2p_{3/2} XPS peak, revealed that as the sum of the Gordy group electronegativity of the R-groups on the β-diketonato ligand increases, the associated binding energy of the Fe 2p_{1/2} peak also increases (see Figure 4). This is to be expected, since the more electron withdrawing the R-group, the more strongly the iron atom will bind to its core electrons, thereby increasing the associated binding energy. The relationship of Fe 2p_{3/2} XPS peak *vs* Gordy group electronegativity, follows the same trend.

Figure 4. ABOUT HERE

Table 1 . ABOUT HERE

The concentration of the amount of iron on the surface was calculated, using the XPS data. From previously published results, it is known that there are ca. 4 – 6 OH groups per nm².²⁶ From the Si 2p XPS data, 1 : 1.97 : 0.48 (29% : 57% : 14%, see Table 1), silane (-O-Si-CH₂-) to -O-Si-OH to -O-Si-O- ratio (see Table 1) implies that there are ca. one -O-Si-CH₂- group for every two -O-Si-OH groups, thus there are ca. 2 – 3 silane molecules per nm². Thus there are 2 – 3 nitrogen atoms per nm². Knowing the ratio between the unbound and bound silanes, as well as the amount of iron present which is the same as the bound silanes, we can determine the amount of Fe per nm² (Table 3). Using surface **1a** as an example: the atomic ratio between the nitrogen and iron is 2.7 : 1 (Table 1) thus 37% of the nitrogen are bound. State otherwise there are 37% iron atoms per nitrogen atoms, thus if there are 2 – 3 nitrogen atoms per nm², there are 37% x (2 – 3) = 0.7 - 1.1 Fe atoms per nm².

It is interesting to note, that the concentration of the iron catalyst (Fe/nm²) on the surface, is related to the electron donating properties of the different β -diketonato ligands as expressed by the sum of the Gordy group electronegativities of the R-groups on the β -diketonato ligands. A higher sum of the Gordy group electronegativities, is associated

with higher iron catalyst loading. A possible explanation could be that as the group electronegativity increases, more electron density is pulled away from the ether-type oxygen, making it more susceptible for the replacement reaction of O of the β -diketonato ligand by the nitrogen on the aminated Si-surface.

Atomic force microscopy (AFM) characterization

AFM has been utilized to investigate the morphology of surfaces **1a-4a** and **6**, as well as of the hydroxylated silicon wafer. The root mean roughness and the surface areas of these surfaces are listed in Table 2, while Figure 5 shows the respective 3D AFM images, performed in contact mode with the various functionalized wafers.

The surface topography of the hydroxylated Si-wafer changed completely, after functionalisation with the 3-aminopropyltrimethoxysilane, **5**, to produce surface **6**. The flat $-\text{Si-OH}$ surface with a few spikes, changed to a very wavy surface with smooth lumps, which do not exhibit defined boundaries. These oblong structures have dimensions of about 50 nm x 250 nm. This shows that instead of just forming a smooth uniform thin layer on the surface, the 3-aminopropyltrimethoxysilane's amino groups tend to aggregate together, probably due to hydrogen bonding. The surface topography changed again, after the different iron tris(β -diketonato) complexes, **1-4**, were anchored onto surface **6**. The new surface structures which formed **1a-4a**, showed a nodular surface with poorly defined grain boundaries. The covalently anchored iron tris(β -diketonato) complexes forms semi-spherical nodes of 50 – 100 nm in diameter. This show that when the iron complexes react with the amino groups of the 3-aminopropyltrimethoxysilane, the oblong structures are broken up into smaller semi-

spherical nodes. The nodes formed by the iron tris(β -diketonato) complexes are smaller than the oblong structures of the 3-aminopropyltrimethoxysilanes, probably due to weaker van der Waals force interaction between the iron tris(β -diketonato) complexes. Surfaces **1a-4a** displayed a root mean square (Rq) roughness of *ca.* 9.04 - 12.28 nm. The three-dimensional data provided by the AFM is important in this study, since these surfaces will be used for catalysis, which will benefit from increased surface area. In this case the surface area and root mean roughness is an indication of accessible the iron centre is for interaction with reagents. It could be argued that the more accessible the iron centre is, the better catalyst the surface would be, however there are other factors that also influence the rate of a reaction.

Figure 5. ABOUT HERE

Table 2. ABOUT HERE

Catalytic testing for the formation of urethane

The catalytic properties of surfaces **1a – 4a** were investigated towards the self-solvating formation of diurethane, to mimic the industrial preparation process of polyurethane, in order to prove that the two-dimensional iron tris(β -diketonato) supported catalysts, can be utilized in the investigation of organic reactions. The catalytic reaction is shown in Scheme 2. This reaction was monitored by ATR FTIR (see Figure 6), following the appearance of the hexamethylenediurethane (product) carbonyl stretching peak at 1691

cm^{-1} , and the disappearance of the cyanate ($-\text{N}=\text{C}=\text{O}$) (reactant) stretching peak of the hexamethylenediisocyanate at 2248 cm^{-1} .

Scheme 2. ABOUT HERE

Figure 6. ABOUT HERE

Table 3 shows the performance data of the catalytic formation of hexamethylenediurethane, from hexamethylenediisocyanate and EtOH, in the presence of the catalyst surfaces, **1a-4a**. The % disappearance of hexamethylenediisocyanate, % appearance of the hexamethylenediurethane and turnover frequency, were determined after 180 min. Data of the homogeneous complexes **1 – 4** is not included and since very little to no product was formed without a catalyst and/or only the Si-wafer. However, all four catalysts which were tested, **1a-4a**, showed the disappearance of the starting materials, namely hexamethylenediisocyanate and EtOH, as well as the formation of the hexamethylenediurethane product, *N,N*-1,6-hexanediybis-*C,C*-diethyl ester.

Table 3. ABOUT HERE

Even though no detailed kinetic study has been conducted, the turnover frequency (TOF) of the catalytic reactions was determined, since this would provide an indication of the catalytic performance of the different model catalysts, **1a-4a**. In the estimation of the TOF, a 0.1 ml solution of 0.22 mol.L⁻¹ hexamethylenediisocyanate (2.2×10^{-5} mol, 1.33×10^{19} molecules) was converted during 180 min (10800 s), to yield the remaining % given in Table 3 for each catalyst. Using catalyst surface **1a** as an example, of the 1.33×10^{19} molecules of hexamethylenediisocyanate present during catalysis, only 50.6% HDI molecules (see Table 3) were converted during 180 min (10800 s), giving the amount of urethane molecules formed as 6.7×10^{18} . From the XPS data, catalyst **1a** has 0.7 - 1.1 active sites (Fe molecules) per nm², thus a total of $1.7 - 2.6 \times 10^{13}$ active sites (as calculated from a catalyst with a total surface area of 0.5 x 0.48 cm; this differs for each catalyst). The TOF was determined using equation (1). For catalyst **1a**, the TOF was determined to be 23 - 37 s⁻¹. From the calculated TOF for catalysts **1a-4a**, in Table 3 and Figure 7, it can be seen that the TOF is dependent on the sum of the Gordy group electronegativities, $\chi_R + \chi_{R'}$, of the R-groups on the β -diketonato ligand of the immobilized iron catalyst. As $\chi_R + \chi_{R'}$ increased, a decrease in TOF was observed. Catalyst **2a** ($\chi_R + \chi_{R'} = 4.42$) gave the highest TOF (33 - 46 s⁻¹), while catalyst **4a** ($\chi_R + \chi_{R'} = 6.01$) had the lowest TOF (16 - 23 s⁻¹). From the AFM discussion it would have been expected that surface **3a** would perform the best since it has the largest surface area and root mean roughness. However, in this case it is clear from the catalysis data that the electronic properties of the catalyst play a far more important factor in determining the TOF than the surface area.

From the Gordy group electronegativities in Table 3 it is evident that an iron centre which is a bit more electron rich, enhances the TOF for the catalytic formation of the hexamethyldiurethane from hexamethylenediisocyanate and ethanol. These two-dimensional model catalysts, with TOF varying from 15- 46 s⁻¹, are much more effective than the homogeneous catalyst Fe(acac)₃, which was investigated in DCM as solvent, to have a TOF of 74.2 h⁻¹ (0.021 s⁻¹),¹⁶ and than catalyst CuCl₂/NaI with a TOF of 1.37 h⁻¹ (3.8 x 10⁻⁴ s⁻¹).³⁶

$$\text{TOF} = \left[\frac{\left(\frac{\text{amount of molecules converted}}{\text{amount of active sites}} \right)}{\text{time in sec}} \right] \quad (\text{Equation 1})$$

Figure 7. ABOUT HERE

The % disappearance of hexamethylenediisocyanate, the % appearance of the hexamethyldiurethane, showed dependence on the sum of the Gordy group electronegativities of the R-groups on the β-diketonato ligands of the iron catalysts. In general, the trend appears to be that, an increase in the sum of the Gordy group electronegativities of the R-groups is accompanied by an increase in the % disappearance of hexamethylenediisocyanate and an increase in the % appearance of the hexamethyldiurethane. This is expected, since the catalyst loading (amount of Fe molecules per nm²) also increased with an increase in the sum of the Gordy group electronegativities of the R-groups. A higher catalyst loading, may, however, lead to a

lower TOF (as was found in this study), since the amount of molecules converted is divided by the amount of active sites (Fe molecules in this study).

Figure 8. ABOUT HERE

In order to test the deactivation and recyclability of catalysts **1a-4a**, a series of eight consecutive catalytic runs was performed. These were all done under the same reaction conditions, while each catalyst was properly washed with ethanol and acetone after each run. The results are presented in Figure 8. The catalytic performance generally stayed fairly constant for the first three cycles, and then gradually started to decrease up to a point, where a 10% decrease in the formation of urethane is observed. This decrease could be contributed either to some leaching of the iron catalyst, or to coking of the catalyst.

4. Conclusion

A series of four different $\text{Fe}(\beta\text{-diketonato})_3$ complexes were covalently anchored onto a flat two-dimensional aminated Si-wafer. Characterisation by XPS revealed that two Gaussian peaks could be fitted into the N 1s peak, belonging to the unreacted amino groups and the amine group. The XPS of the fluorine-containing catalysts (**3a** and **4a**) showed that more than one Gaussian peak could be fitted into the F 1s peaks, which was attributed to the CF_3 group either being bound to the ether bond ($-\text{O}-\text{C}-\text{CF}_3$) or to the amine bond ($-\text{N}-\text{C}-\text{CF}_3$). The XPS revealed that the binding energy of the Fe $2p_{3/2}$ peaks are dependent on the sum of the Gordy group electronegativities of the R-groups on the

β -diketonato ligands. The atomic ratios obtained from the XPS data, were used to calculate the iron concentration on the surface, which was found to be *ca.* 0.5 – 2.7 Fe atoms per nm², depending on the catalyst used. AFM revealed the topography of the catalyst surface to be nodular, with poorly defined grain boundaries.

The catalytic activity of the different immobilized iron catalysts, for the formation of hexamethylenediurethane from hexamethylenediisocyanate and ethanol, was tested. The iron tris(β -diketonato) immobilized catalyst, with β -diketonato = dbm, which possessed the lowest sum of the Gordy group electronegativities of the R-groups on the β -diketonato ligand, showed the highest TOF (33 - 46 s⁻¹) for the catalytic formation of the diurethane. It can thus be concluded, that the more electron rich the iron centre, the higher the catalytic activity of the catalyst.

Supplementary Information

XPS spectra of surfaces 1a-4a.

Acknowledgements

The authors acknowledge financial support from SASOL, South African National Research Foundation and the UFS, during the course of this study.

¹ E. Erasmus, P.C. Thüne, M.W.G.M. (Tiny) Verhoeven, J.W. Niemantsverdriet, J.C. Swarts, *Cat.Comm.* 27 (2012) 193.

² a) E. Erasmus, J.W. Niemantsverdriet, J.C. Swarts, *Langmuir*, 2012, 28, 16477-16484.

b) E. Erasmus, *S. Afr. J. Chem.*, 2013, 66, 216-220.

- ³ C. Merckle, J. Blumel, *Topics Catal.* 34 (2005) 5.
- ⁴ a) M. Trzebiatowska-Gusowska, A. Gagor, E. Coetsee, E. Erasmus, J.C. Swarts, J. *Organomet. Chem.* 393-403 (2013) 745.
- b) R.K. Sharma, C. Sharma, *J. Macromol. Sci., Part A: Pure Appl. Chem.* 48 (2011) 155.
- c) T. Shamim, M. Gupta, S. Paul, *J. Mol. Catal. A: Chem.* 302 (2009) 15.
- d) R.K. Sodhi, S. Paul, J.H. Clark, *Green Chem.* 14 (2012) 1649.
- ⁵ a) F. Piestert, R. Fetouaki, M. Bogza, T. Oeser, J. Blumel, *Chem. Comm.* (2005) 1481.
- b) T. Posset, J. Blumel, *J. Amer. Chem. Soc.* 128 (2008) 8394.
- c) J. Blumel, *Coord. Chem. Rev.* 252 (2008) 2410-2423.
- ⁶ Q.J. Miao, Z.P. Fang, G.P. Cai, *Catal. Comm.* 4 (2003) 637.
- ⁷ J.M. Richardson, C.W. Jones, *J. Catal.* 251 (2007) 80.
- ⁸ a) J.C. Swarts, M.A.S. Aquino, J.-Y. Han, K.-Y. Lam and A.G. Sykes, *Biochim. Biophys. Acta*, (1995) 215.
- b) J.-Y. Han, J.C. Swarts and A.G. Sykes, *Inorg. Chem.*, 35, 4629-4634 (1996).
- ⁹ J. Conradie, A. Ghosh, *Inorg. Chem.*, 45, (2006) 4902.
- ¹⁰ S. Basu, R. Grubina, J. Huang, J. Conradie, Z. Huang, A. Jeffers, A. Jiang, X. He, I. Azarov, R. Seibert, A. Mehta, R. Patel, S.B. King, N. Hogg, A. Ghosh, M.T. Gladwin, D.B. Kim-Shapiro, *Nat. Chem. Biol.* 2007, 3, 785.
- ¹¹ B.M. Bocknack, L.C. Wang, F.W. Hughes, M.J. Krische, *Tetrahedron*, 61 (2005) 6266.
- ¹² R. Varala, A. Nasreen, S.R. Adapa, *Can. J. Chem.* 85 (2007) 148.
- ¹³ P.S. Umare, G.L. Tembe, *React. Kinet. Catal. Lett.* 82 (2004) 173.
- ¹⁴ R.K. Sodhi, S. Paul, *Catal. Lett.* 141 (2011) 608.
- ¹⁵ V. De Lima, N. Da Silva Pelissoli, J. Dullius, R. Ligabue, S. Einloft, *J. Appl. Poly. Sci.* 115 (2010) 1797.
- ¹⁶ R.A. Ligabue, A.L. Monteiro, R.F. de Souza, M.O. de Souza, *J. Mol. Catal. A; Chem.*, 130 (1998) 101.
- ¹⁷ F. Moulder, W.F. Stickle, P.E. Sobol, K.D. Bomben, *Handbook of X-ray Photoelectron Spectroscopy*, ULVAC-PHI, Inc., 370 Enzo, Chigasaki 253-8522, Japan, 368 1995, pp. 45, 57, 143.

- ¹⁸ M.M. Conradie, P.H. van Rooyen, J. Conradie, *J. Mol. Struct.* 1053 (2013) 134.
- ¹⁹ a) E.W. Berg, J.T. Truemper, *J. Phys. Chem.* 1960 (64) 487.
b) K. Endo, M. Furukawa, H. Yamatera, H Sano, *Bull. Chem. Soc. Jpn* 1980 (53) 407
c) G.S. Hammond, D.C. Nonhebel, C.S. Wu, *Inorg. Chem.* **1963** (2) 73.
- ²⁰ E.W. Berg, J.T. Truemper, *J. Phys. Chem.* **1960** (64) 487.
- ²¹ M.-L. Hu, Z.-M. Jin, Q. Miao, L.-P. Fang, *Z. Kristallogr. - New Cryst. Struct.* **2001** (216) 597.
- ²² B. Kaitner, B. Kamenar, *Cryst. Struct. Commun.* **1980** (9) 487.
- ²³ I.A. Baidina, P.A. Stabnikov, I.K. Igumenov, S.V. Borisov, *Koord. Khim. (Russ.) (Coord. Chem.)* **1986** (12) 258.
- ²⁴ I.A. Baidina, P.A. Stabnikov, I.K. Igumenov, S.V. Borisov, *Koord. Khim. (Russ.) (Coord. Chem.)* **1986** (12) 404.
- ²⁵ C.E. Pfluger, P.S. Haradem, *Inorg. Chim. Acta* **1983** (69) 141.
- ²⁶ J.W. Niemantsverdriet, A.F.P. Engelen, A.M. de Jong, W. Wieldraaijer, G.J. Kramer, *Appl. Surf. Sci.* 144-145 (1999) 366-374.
- ²⁷ L.T. Zhuravlev, *Langmuir* 316 (1987). 316
- ²⁸ J. Kim, P. Seidler, L.S. Wan, C. Fill, *J. Colloid Interface Sci.* 329 (2009) 114.
- ²⁹ T.G. Vargo, J.A. Gardella Jr., *J. Vac. Sci. Technol. A*, A7 (1989) 1733.
- ³⁰ Y.L. Yan, M.A. Helfand, C.R. Clayton, *Appl. Surf. Sci.* 37 (1989) 395.
- ³¹ J.M. Lindquist, J.P. Ziegler, J.C. Hemminger, *Surf. Sci.* 210 (1989) 27.
- ³² S. Rangan, F. Bournel, J.J. Gallet, S. Kubsky, K. Le Guen, G. Dufour, F. Rochet, F. Sirotti, G. Piaszenski, R. Funke, M. Knepe, U. Köhler, *J. Phys. Chem. B*, 109 (2005) 12899.
- ³³ a) W.C. du Plessis, T.G. Vosloo, J.C. Swarts, *Dalton* (1998) 2507.
b) R.E. Kagarise, *J. Am. Chem. Soc.* 77 (1955) 1377.
c) W.C. du Plessis, J.J.C. Erasmus, G.J. Lamprecht, J. Conradie, T.S. Cameron, M.A.S. Aquino, and J.C. Swarts, *Can. J. Chem.* 77 (1999) 378.
- ³⁴ a) E. Erasmus, J. Conradie, A. Muller, J.C. Swarts, *Inorg. Chim. Acta* 360 (2007) 2277.
b) E. Erasmus, *Inorg. Chim. Acta* 378 (2011) 95.
c) T.J. Muller, J. Conradie, E. Erasmus, *Polyhedron* 33 (2012) 257.

-
- d) K.C. Kemp, E. Fourie, J. Conradie, J.C. Swarts, *Organometallics* 27 (2008) 353.
- e) J.J.C. Erasmus, J. Conradie, *Electro Chim. Acta*, 56 (2011) 9287.
- f) M.M. Conradie, A.J. Muller, J. Conradie, *S. Afr. J. Chem.* 61 (2008) 13.
- g) J. Conradie, J.C. Swarts, *Dalton Trans.* 40 (2011) 5844.
- h) A. Kuhn, K.G. von Eschwege, J. Conradie, *Electro Chim. Acta*, 56 (2011) 6211.
- i) J. Conradie, *J Organomet. Chem* 719 (2012) 8.
- j) J. Conradie, *Inorg. Chim. Acta* 392 (2012) 30.
- ³⁵ L. Pauling, *J. Amer. Chem. Soc.* 54 (1932) 3570.
- ³⁶ B. Chen, S.S.C. Chuang, *Green Chem.* 5 (2005) 484.

ACCEPTED MANUSCRIPT

Figures and Schemes

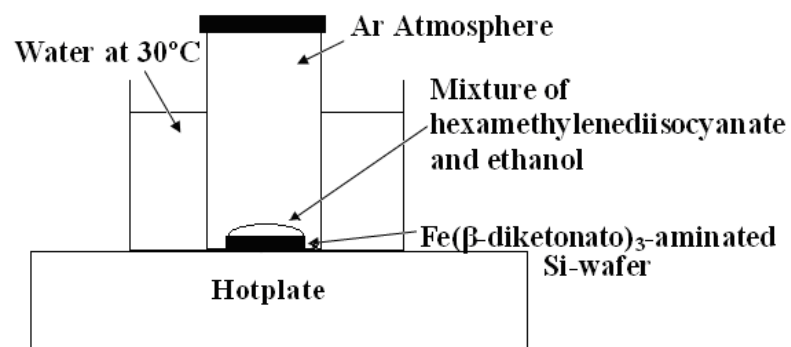
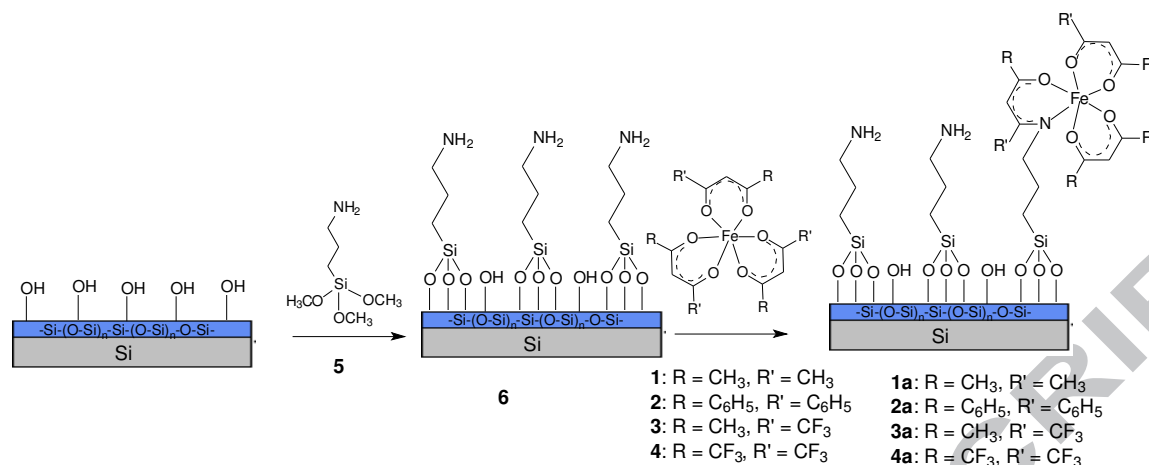


Figure 1. Schematic representation of the reaction vessel.



Scheme 1. The functionalization of the aminated Si wafers, surface **6**, with four [Fe(β -diketonato)₃] complexes (**1-4**), producing surfaces (**1a-4a**). The gray layer at the bottom is Si-metal, while the blue layer on top of it consists of -O-Si-O-.

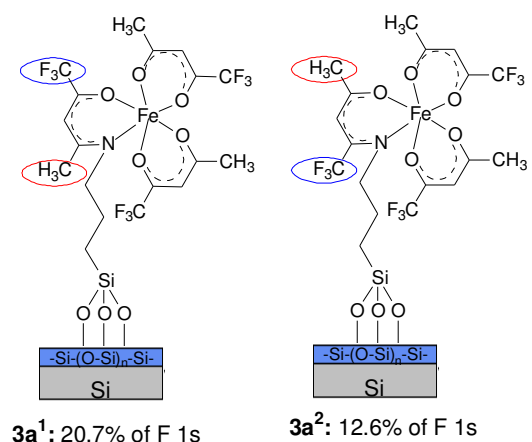


Figure 2. Schematic representation of the different binding possibilities of $\text{Fe}(\text{CF}_3\text{COCHCOCH}_3)_3$ to the aminated surface, which could either be adjacent to the $-\text{CH}_3$ or $-\text{CF}_3$ group on the ligand.

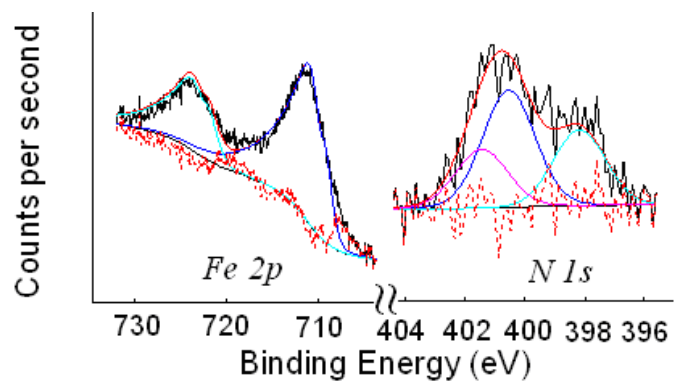


Figure 3. Detailed XPS spectra of Fe 2p ($2p_{3/2}$ peak at 710.75 eV and $2p_{1/2}$ peak at 724.70 eV) and N 1s (unbound N at 401.95 eV, bound N at 398.65 and 401.03 eV), of surface **3a**.

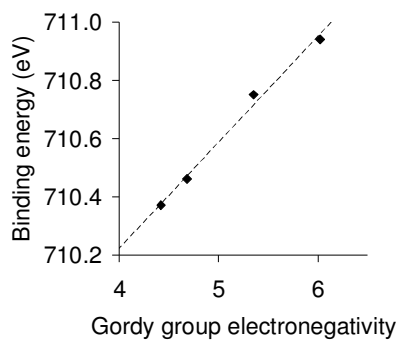
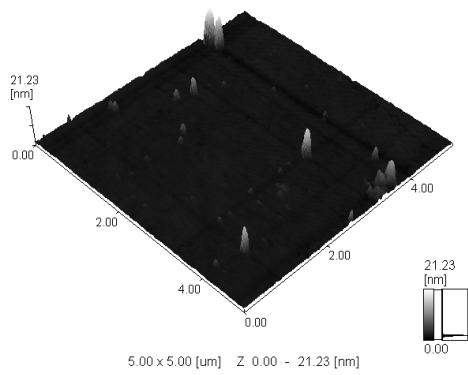
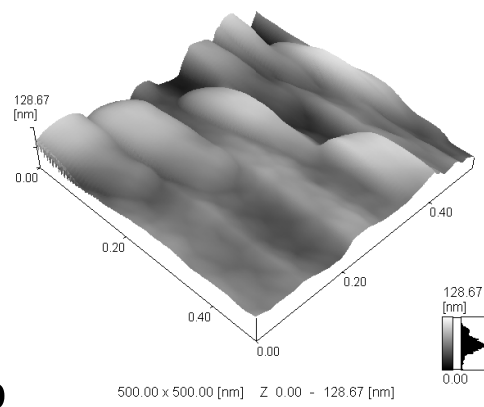


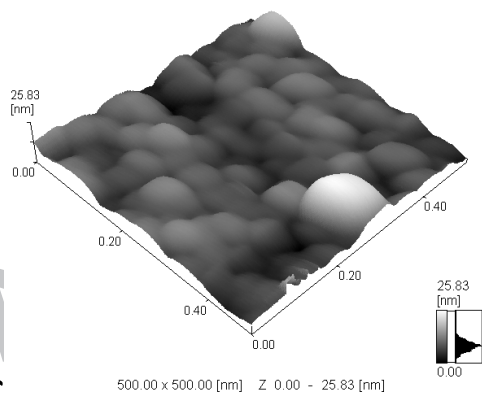
Figure 4. Graph of the sum of the Gordy Group electronegativities of the R-groups on the β -diketonato ligand of **1a** – **4a** vs binding energy, of the bound Fe $2p_{3/2}$ XPS peak.



a



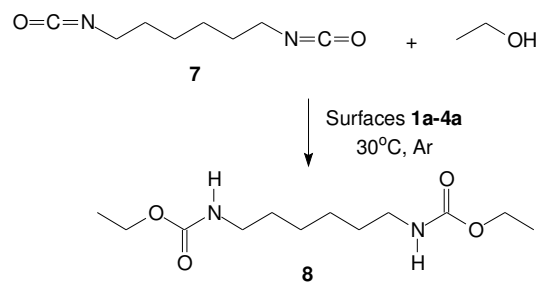
b



c

Figure 5. Three dimensional images as obtained from AFM of (a) the hydrophilic hydroxylated Si-wafer, (b) the aminated silicon surface **6**, and (c) surface **2a**, as a representative of the four catalyst surfaces containing the iron complexes.

ACCEPTED MANUSCRIPT



Scheme 2. Schematic representation of the catalytic formation, via surfaces **1a-4a**, of the hexamethylenediurethane, **8**, from hexamethylenediisocyanate, **7**, and EtOH, using a ten times excess of EtOH in a self-solvating reaction.

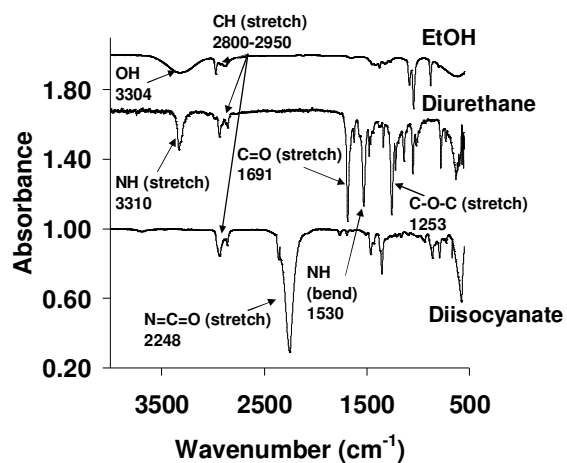


Figure 6. ATR FTIR spectra of EtOH (reactant, top), the hexamethylenediurethane (product, middle) and hexamethylenediisocyanate (reactant, bottom).

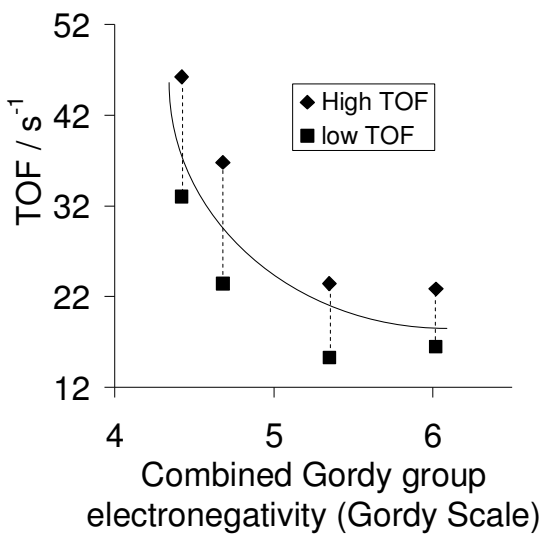


Figure 7. Graph of the sum of the Gordy group electronegativities of the R-groups on the β -diketonato ligand of **1a** – **4a**, vs the TOF of surface catalysts **1a-4a**.

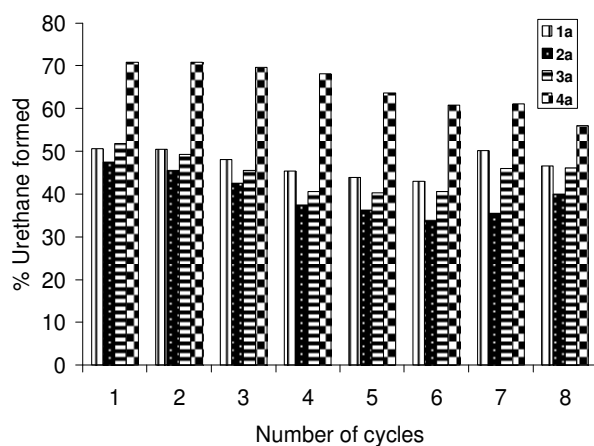


Figure 8. Yields of the batch-wise catalytic formation of the diurethane, using surface catalysts **1a-4a**, for eight cycles.

Tables

Table 1. The concentration of the Fe on the Si-surfaces and binding energies in eV, for N, Si, F and the Fe center, derived from XPS measurements. (AR = atomic ratios obtained from detailed XPS scans)

Compound	$\chi_R + \chi_R^a$	N 1s	F 1s	Si 2p	Fe 2p _{3/2}	Fe 2p _{1/2}	Fe molecules per nm ²
1a	4.68	399.36 ^b (37%) ^j	-	100.74 (29%) ^l	710.46	724.41	0.7-1.1
Fe(acac)₃		401.73 ^c (63%)	-	102.56 (57%) ^m	-	-	-
				103.65 (14%) ⁿ			
AR^k		2.7	-	8.3	1	-	-
2a	4.42	399.85 ^b (27%) ^j	-	101.54 (29%) ^l	710.37	724.32	0.5-0.7
Fe(dbm)₃		401.15 ^c (76%)	-	102.58 (57%) ^m	-	-	-
				103.57 (14%) ⁿ			
AR^k		4.1	-	5.3	1	-	-
3a	5.35	398.65 ^b (29%) ^j	684.63 ^e (13%)	101.64 (29%) ^l	710.75	724.70	1.5-2.3
Fe(tfaa)₃		401.03 ^d (47%) ^j	686.24 ^h (21%)	102.78 (57%) ^m	-	-	-
		401.95 ^c (24%)	688.52 ⁱ (67%)	103.83 (14%) ⁿ	-	-	-
AR^k		1.3	3.2	6.65	1	-	-
4a	6.02	399.91 ^b (91%) ^j	684.69 ^e (17%)	101.60 (29%) ^l	710.94	724.89	1.8-2.7
Fe(hfaa)₃		402.72 ^c (9%)	688.27 ⁱ (83%)	102.53 (57%) ^m	-	-	-
				103.47 (14%) ⁿ			
AR^k		1.1	7	5.5	1	-	-

a) The group electronegativity ($\chi_R + \chi_R^a$) is calculated on the Gordy scale, with $\chi_{CF_3} = 3.01$, $\chi_{CH_3} = 2.34$ and $\chi_{Ph} = 2.21$.³⁷

b) Bound nitrogen (-N-C-CH₃ for **1a**, -N-C-Ph for **2a**, -N-C-CH₃ for **3a**, -N-C-CF₃ for **4a**)

c) Unbound nitrogen (-NH₂)

d) Bound nitrogen (-N-C-CF₃ for **3a**)

- e) -N-C-CF₃
- f) -O-C-CF₃
- g) CH₃-(O)-C-CH-C-(N)-CF₃
- h) CH₃-(N)-C-CH-C-(O)-CF₃
- i) CH₃-(O)-C-CH-C-(O)-CF₃
- j) % of the bound nitrogen relative to the % of the unbound nitrogen
- k) Atomic ratios were obtained from the XPS wide scan
- l) -O-Si-CH₂- of the silane
- m) -O-Si-OH on the surface
- n) -O-Si-O- of the surface

Table 2. The root mean roughness (Rq) and surface area, of surface **1a-4a, 6** and the hydroxylated Si-wafer, as estimated by AFM.

Surface	Root Mean roughness (Rq)	Surface area (μm ²)
Si-wafer	0.75	0.259
6	12.39	0.283
1a	10.93	0.275
2a	9.04	0.257
3a	12.28	0.279
4a	9.04	0.260

Table 3. Performance data of the four catalyst surfaces: The combined Gordy group electronegativity ($\chi_R + \chi_R$), the amount of Fe-molecules per square nm, the total amount of Fe-molecules per surface, turnover frequency (TOF in s^{-1}), % disappearance of hexamethylenediisocyanate after 180 min (% HDI), % appearance of the hexamethylenediurethane product (% HDU) after 180 min

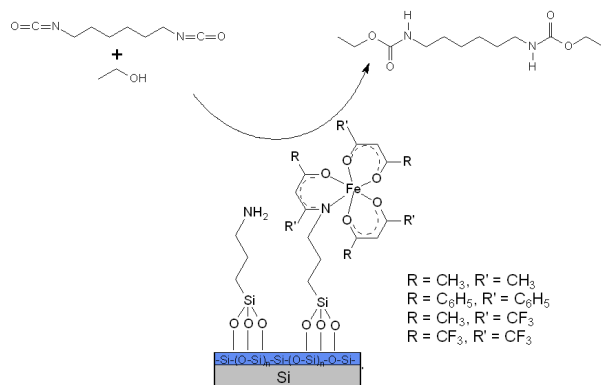
	$\chi_R + \chi_R^a$	Fe molecules per nm^2^b	Fe molecules $\times 10^{-13}$ per surface ^c	TOF (s^{-1})	% Disappearance of HDI	% Appearance of HDU
1a	4.68	0.7 – 1.1	1.7 – 2.6	23-37	49.6	50.6
2a	4.42	0.5 – 0.7	1.3 – 1.8	33-46	47.3	47.3
3a	5.35	1.5 – 2.3	2.7 – 4.1	15-24	50.6	51.8
4a	6.02	1.8 – 2.7	3.8 – 5.7	16-23	70.4	70.7

a) The group electronegativity ($\chi_R + \chi_R$) is calculated on the Gordy scale with $\chi_{CF_3} = 3.01$, $\chi_{CH_3} = 2.34$, $\chi_{Ph} = 2.21$.³⁷

b) Using surface **1a** as an example: the atomic ratio between the nitrogen and iron is 2.7 : 1 (Table 1) thus 1 of every 2.7 or 37% of the nitrogen are bound. State otherwise there are 37% iron atoms per nitrogen atoms, thus if there are 2 – 3 nitrogen atoms per nm^2 , there are $37\% \times (2 - 3) = 0.7 - 1.1$ Fe atoms per nm^2 .

c) To calculate the total Fe molecules per surface, the amount of Fe per nm^2 was multiplied by the total surface area in nm^2 . Using surface **1a** as an example: $(0.7 - 1.1 \text{ Fe atoms per } nm^2) \times 2.4 \times 10^{13} \text{ } nm^2 = 1.7 - 2.6 \times 10^{13}$ Fe molecules per surface. The surface for each sample was measure individually to be: $1a = 2.4 \times 10^{13} \text{ } nm^2$, $2a = 2.6 \times 10^{13} \text{ } nm^2$, $3a = 1.8 \times 10^{13} \text{ } nm^2$, $4a = 2.1 \times 10^{13} \text{ } nm^2$.

Pictogram for Table of contents



Synopsis for Table of contents

A series of immobilized $\text{Fe}(\beta\text{-diketonato})_3$ on Si-wafers were prepared, and tested for their catalytic activity in the heterogeneous phase for the formation of diurethane. It was found that more electron donating R-groups on the β -diketonato ligand (RCOCHCOR) increases the catalytic activity.